ORIGINAL RESEARCH

A Ferritin-Based Eg95 Nanoparticle Vaccine Adjuvanted with pCpG Eliciting Robust Immune Responses Against Cystic Echinococcosis in Mice Model

Xintao Gao[1,*], Xizhou Zhu[2,*], Xingjian Liu[1], Chenghao Zhou[1], Yuting Shang[1], Tong Wu[1], Hong Jia[3], Zhifang Zhang[1], Yinü Li[1], Ting Xin[3]

[1]National Key Laboratory of Agricultural Microbiology, Biotechnology Research Institute, Chinese Academy of Agricultural Sciences, Beijing, People's Republic of China; [2]Bioproducts Engineering Center, Chinese Academy of Agricultural Sciences, Beijing, People's Republic of China; [3]Institute of Animal Sciences, Chinese Academy of Agricultural Sciences, Beijing, People's Republic of China

*These authors contributed equally to this work

Correspondence: Ting Xin; Yinü Li, Email xinting@caas.cn; liyinv@caas.cn

Introduction: Cystic echinococcosis (CE), a chronic disabling parasitic zoonosis, poses a great threat to public health and livestock production and causes huge economic losses globally. The commercial Quil-A-adjuvanted Eg95 vaccine was empirically effective for CE control; however, it is expensive and has side effects and insufficient immunity.

Purpose: This study aimed to employ a novel adjuvant consisting of a delivery system and an immune potentiator and assess its adjuvanticity to Eg95 antigen, thereby developing a safe and cost-effective novel vaccine against the disease.

Methods: A ferritin-based Eg95 nanoparticle antigen was prepared and then mixed with a plasmid containing the TLR9 agonist CpG to formulate a novel nanovaccine. The safety and efficacy of the vaccine were evaluated in vitro and in vivo.

Results: The nanovaccine induced potent and enduring Eg95-specific humoral and cellular immune responses, as well as protective immunity-associated Th1 polarization supported by the higher ratios of IgG2a/IgG1 and IFN-γ/IL-4. Meanwhile, this nanovaccines exhibited favorable safety and economic profiles.

Conclusion: Our data demonstrated that the ferritin-CpG hybrid is a promising combination adjuvant to upgrade the traditional Quil-A and this combination adjuvant-based nanovaccine presents good potential as an alternative to the commercial one for practical CE control.

Keywords: cystic echinococcosis, vaccine, combination adjuvant, ferritin nanoparticle, CpG

Introduction

Cystic Echinococcosis (CE) adversely affects humans and various animal species and is a neglected parasitic zoonosis.[1] The causative agent of the disease is the larvae of cestodes (tapeworms) of *Echinococcus granulosus (E. granulosus) sensu lato (s.l).* (genus *Echinococcus*, family Taeniidae) consisting of ten strains/genotypes (G1-G10) divided into five species including *E. granulosus sensu stricto (s.s).*, *Echinococcus equinus, Echinococcus ortleppi, Echinococcus canadensis, and Echinococcus felidis*.[2,3] *E. granulosus s.l.* is most widely distributed in pastoral and tropical areas, of which, *E. granulosus s.s.* (sheep strain, G1-G3) is cosmopolitan, with other species being focal in Eurasia/America/Africa.[4] The life cycles of *E. granulosus s.l.* are complicated and rely on a predator–prey relationship in which carnivores (canids and felines) act as definitive hosts, and their herbivorous prey serve as intermediate hosts (ungulates, rodents, and lagomorphs); humans are accidentally infected through fecal-oral contact with proglottids and eggs in dogs' feces, rather than directly involved in the parasite life cycle.

Graphical Abstract
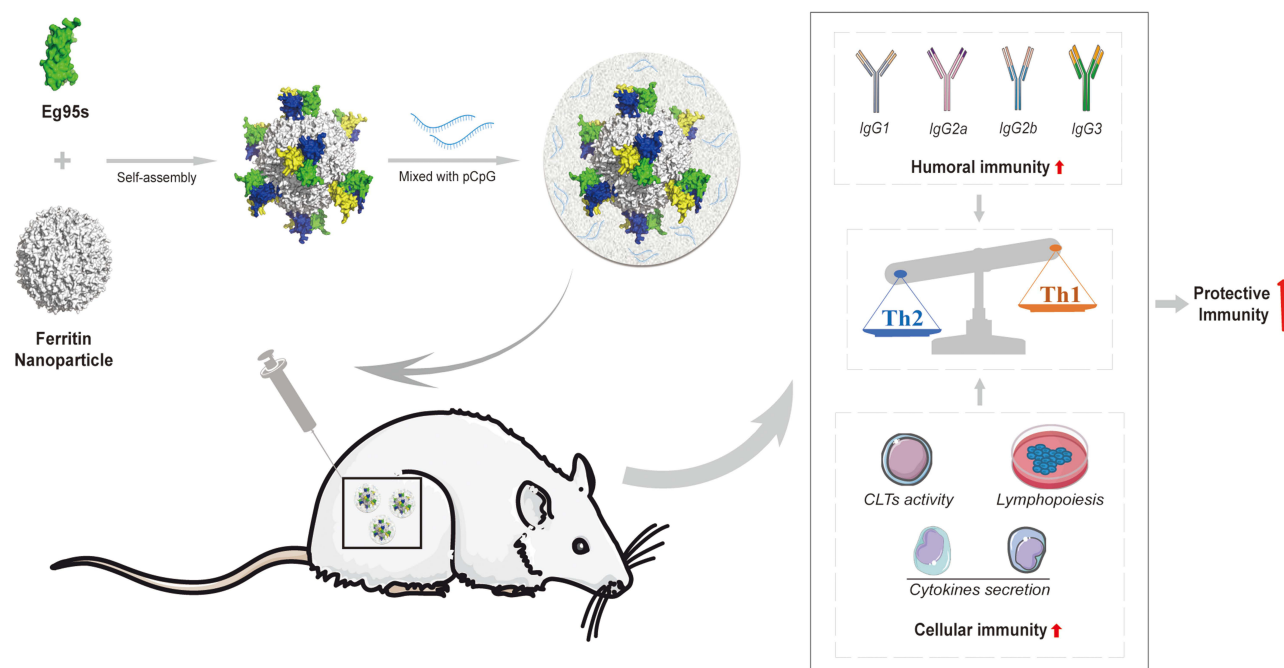
Globally, this disease has caused over one million disability-adjusted life years (DALYs) in humans and has been jeopardizing the livestock industry, bringing over $3 billion in corresponding annual losses to treatment and livestock production.[5] Domestically, China is one of the most epidemic countries for CE, and the disease has emerged in as many as 375 districts/counties with a north- and west-focused epidemic distribution zone (Figure 1), accounting for 40% of the global burden.[6] The disease is listed as one of the 20 neglected diseases targeted for control or elimination by 2050 on the WHO's roadmap (http://whqlibdoc.who.int/hq/2012/WHO_HTM_NTD_2012.1_eng.pdf). in and by 2030 in "Healthy China 2030".[7] However, due to the complexity of the life cycle and extensive genetic diversity, the comprehensive prevention and control of the disease still face many difficulties, making the task urgent and challenging.

Vaccines remain one of the most cost-effective ways to prevent and control this disease. Hitherto, the only validated protective antigen is the oncosphere stage-derived Eg95,[8] and a commercial vaccine formulated with Eg95 and Quil-A adjuvant has shown good protective immunity against livestock (eg, sheep and cattle). This intermediate host-targeted Eg95 vaccine has been used in countries (eg, South America, Australia, and China) as a powerful complementary intervention to eliminate CE transmission.[4] In China, the vaccine has been included in the national compulsory immunization program since 2017, and its protective effect and positive efficacy have been widely confirmed in the field. Nevertheless, the adjuvant Quil-A used in this vaccine formulation has high cost and high side effects such as hemolysis; meanwhile, the immunization procedure "two injections within one year and annual booster" is difficult and costly to implement well for grazing animals, resulting in invalid vaccination in practice, which has significant side effects on CE control.[7] Access to more preferred and economical adjuvants aiding for Eg95 antigen to enhance the durability and breadth of immune response to improve the benefit/cost ratio seems to be a reasonable and sustainable solution.

Ferritin (Fe), which contains 24 subunits of identical or two different types (light and heavy), is a spherical iron storage protein assembled from eight units, each with three-fold axis symmetry.[9] The characteristics of native ferritin nanocages, such as their unique structure and excellent safety profile, make ferritin-based formulations have great application potential for drug delivery, biosensing, imaging,[10] and generation of chimeric nanoparticles with surface-exposed arrays of immunogenic epitopes or proteins,[11,12] which elicit an effective immune response more intensely,
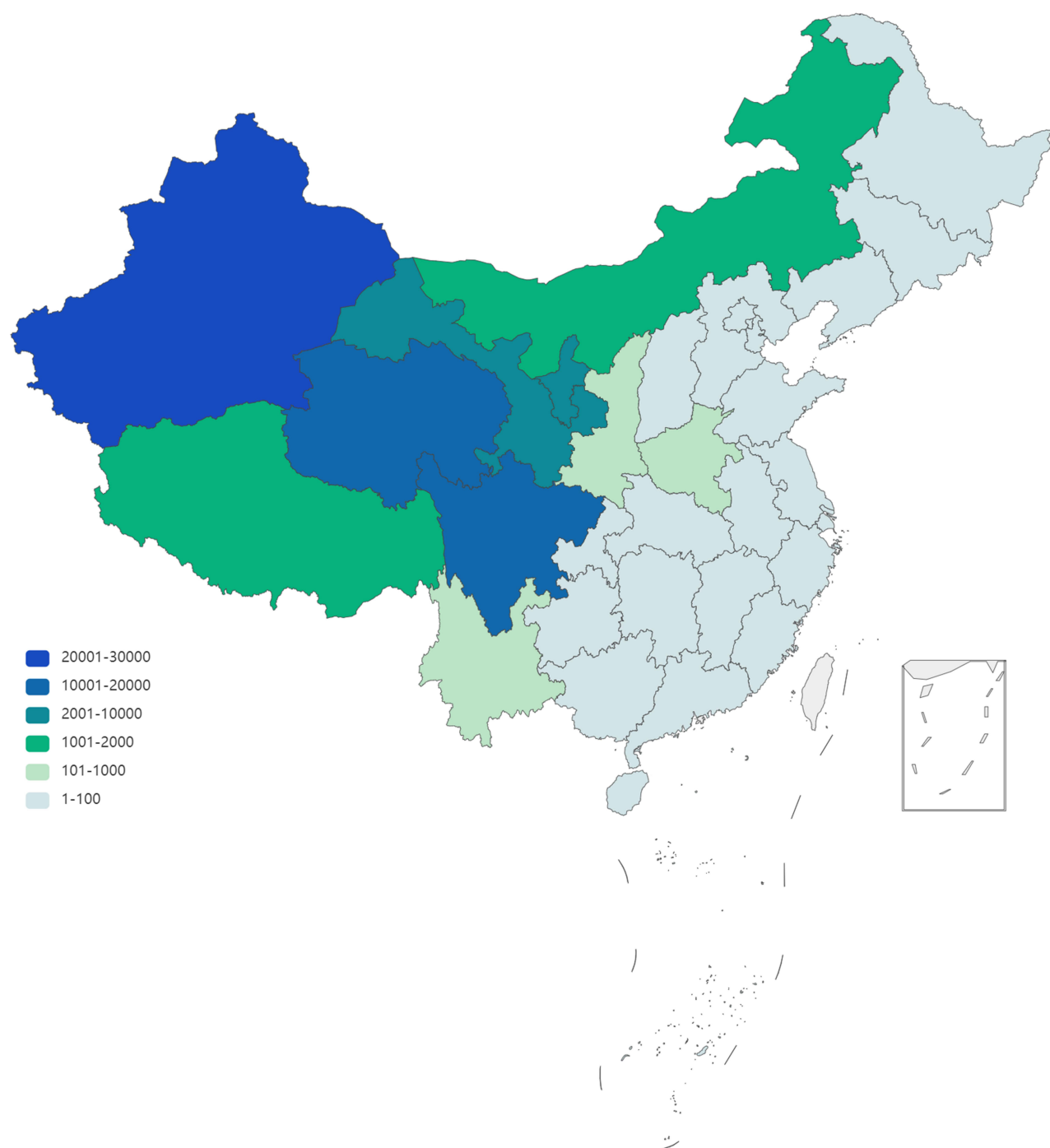
Figure 1 Human CE cases distribution in China. The figure was drawn by the Python, and the data used was the reported cases of echinococcosis in China from 2004 to 2023.

making the ferritin-based delivery system a promising recombinant subunit vaccine development platform. This strategy has been extensively applied in the development of vaccines against HIV,[13] influenza,[14] Epstein–Barr virus,[15] and SARS/ MERS-CoV.[16–18]

However, the application of ferritin for the delivery of monomeric antigen Eg95 has not been reported to date. Whether there is a synergistic enhancement effect of the combination adjuvant comprising the delivery system ferritin and the TLR-9 potentiator CpG to Eg95 is uncertain; further, the effect of ferritin-based formulation coupled with CpG

on the quantity and quality of humoral and cellular immune responses elicited by Eg95 antigen remains unknown. In this study, a ferritin-based Eg95 nanoparticle antigen was rationally engineered and genetically prepared using *E. coli*, and this purified, self-assembled antigen was mixed with a low-cost derivative of CpG to formulate a novel nanovaccine. The efficacy of the vaccine was comprehensively evaluated and compared to that of the traditional commercial vaccine using several immune parameters, including serum antibody titers, cytotoxic T lymphocytes (CTLs) activity, cytokine responses, and lymphocyte proliferation. In this study, the Ferritin-CpG hybrid as a promising combination adjuvant to upgrade the traditional Quil-A was demonstrated, and this adjuvant-based nanovaccine presents good application potential in the practical of CE control by improving the benefit/cost ratio.

Materials and Methods
Adjuvants, Antigens and Animals
Adjuvants
Quil-A adjuvant was purchased from InvivoGen (San Diego, CA). The pUC-18 vector containing 20 copies of CpG ODN 2006 (sequence: 5′-TCGTCGTTTTGTCGTTTTGTCGTT-3′) (pCpG) was constructed in our laboratory, and the pUC18-CpG adjuvant at a concentration of 2 mg/mL was obtained through fermentation, purification and endotoxin removal[19,20] for vaccine formulation.

Expression and Purification of Eg95 and Eg95-Ferritin
All the targeted sequences were synthesized by GenScript Biotech Co., Ltd. (Nanjing, China). The truncated sequence Eg95s (14–129 aa) was extracted from the wild-type sequence of the *Eg95* gene (GenBank: X90928.1) and cloned into pGEX-6p-1, expressed with a GST tag at the N-terminus in *E. coli* BL21 (Eg95s-GST), which was purified by affinity chromatography (Glutathione Sepharose 4 B, Cytiva, Germany) and cleaved the GST tag by HRV 3C protease (Thermofisher). The protein removed GST tag was termed as Eg95s then purified by ion-exchange chromatography (HiTrap Capto SP ImpRes column, Cytiva, Germany) and size-exclusion chromatography (Superdex 75 10/300 GL column, Cytiva, Germany).

The purified proteins were exchanged with sterile phosphate-buffered saline (PBS) using a HiPrep 26/10 desalting column (Cytiva, Germany). Eg95s were linked to *Helicobacter pylori* ferritin (RefSeq: WP_000949190.1, 5–167 aa, N19Q) by the flexible linker SGG,[21] and cloned into the pET-28a expression vector, which was transformed into *E. coli* BL21 (DE3) cells. Eg95s-Fe was mainly expressed in the form of inclusion bodies, purified using BeyoGold™ His-tag Purification Resin (P2233) (Beyotime, Shanghai, China) after 8M urea denaturation, and then reconstituted and desalted using gradient dialysis.

All purified proteins were subjected to endotoxin removal twice using Triton X-114 two-phase separation and tested using the chromogenic end-point Tachypleus amebocyte lysate method (Chinese Horseshoe Crab Reagent Manufactory, Co., Ltd., China). After filtration through a 0.22 μm sterile filter membrane, all proteins were confirmed by 12% SDS-PAGE and Western blotting. With reference to the previous method,[22] nanoparticle samples were negatively stained with 2% uranyl acetate and observed using a transmission electron microscopy (TEM) (HITACHI TEM-H7500); meanwhile, the size of Eg95s-Fe nanoparticles was calculated by Image J and their distribution was analyzed using the methods of Descriptive Statistics and Gaussian fitting in the Origin software. Immunogold labeling was used to perform the immunoelectron microscopy (IEM) observation. In the case, the polyclonal antibody obtained from the mice vaccinated with ferritin (1:50 dilution) and goat Anti-mouse gold-10nm IgG (Abcam, ab270536) (1:100 dilution) was employed as the primary and secondary antibody, respectively. TEM was used to observe and confirm whether the Eg95s-Fe nanoparticles were successfully assembled, and immunoelectron microscopy (IEM) was used to identify whether Eg95s were displayed on the surface of the nanoparticles. Protein concentrations were determined using a Pierce BCA Protein Assay Kit (Thermo Fisher Scientific, USA), according to the manufacturer's instructions. All purified proteins were diluted to a final concentration of 2 mg/mL in sterile PBS (pH 7.4) and stored at −80 °C.

Animals

BALB/c female mice (6–8 weeks old) were obtained from Vital River Laboratory Animal Technology Co., Ltd. (Beijing, China), and animal experiments were performed in the laboratory animal room of the Institute of Animal Sciences of the Chinese Academy of Agricultural Sciences (IAS-CAAS). Animal experiments were performed according to the Regulation of the People's Republic of China on the Administration of Laboratory Animals and approved by the Animal Care and Use Committee of IAS-CAAS (approval number: IAS-2024-107).

Vaccine Formulation

The vaccines used in this study were prepared according to the production standards of Chongqing AULEON Biologicals Co., Ltd. (Chongqing, China). One dosage of different components for mouse studies was 15 μg soluble antigen (Eg95s) or 37.5 μg Eg95s-Fe (equal amount of molar molecular weight to Eg95s), 10 μg pCpG and 15 μg Quil-A, respectively. Five batches of vaccines, Eg95s, Eg95s+Quil-A, Eg95s+pCpG, Eg95s-Fe, and Eg95s-Fe+pCpG, were formulated and visualized, as shown in Figure 2.
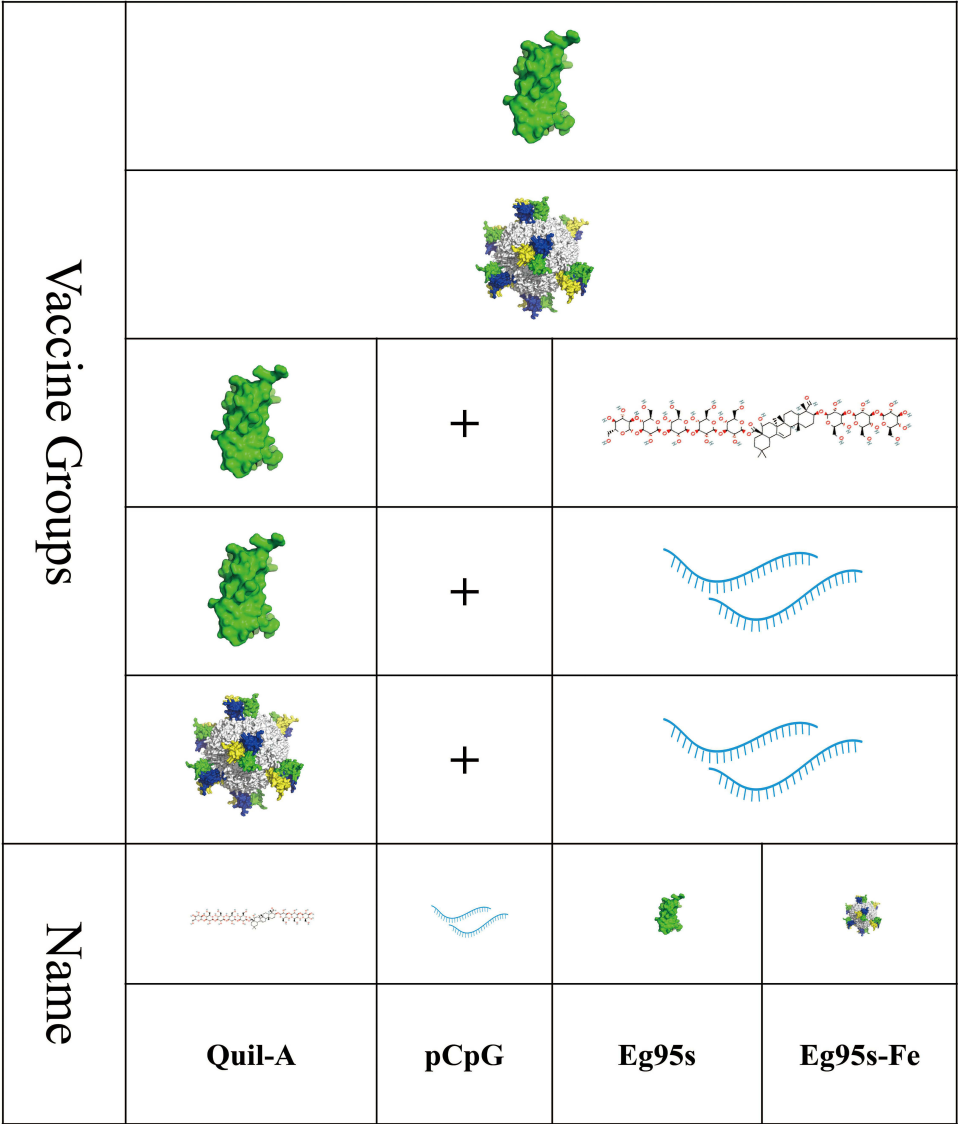

Figure 2 Schematic diagram of vaccine formulation.

Safety Evaluation in vitro

MTS Assays for Cytotoxicity Analysis

The cytotoxicity was analyzed by MTS assay.[23] Briefly, RAW 264.7 cells (ATCC, TIB-71), MDBK cells (ATCC, CCL-22), and BHK-21 cells (ATCC, CCL-10) were seeded into 96-well culture plates (1×10^4 cells per well). After cell attachment, the samples were diluted with RPMI1640 to 4 mg/mL and then diluted with the same cell culture medium. Ten microliters of different concentrations of samples were added to cells and incubated for 24 h at 37 °C under 5% CO_2. Next, 10 μL of MTS stock solution was added to each well and incubated for another 3 h under the same conditions. Finally, absorbance was measured at 490 nm using a microplate reader (ELX800 UV, BIO-TEK, USA). Cell viability was quantified using the following formula: Cell viability%= $(OD_{exp} - OD_{blank}) / (OD_{control} - OD_{blank}) \times 100\%$ (OD_{exp}: the optical density of the cells exposed to adjuvant dilution; OD_{blank}: the optical density of the cells exposed to medium; OD_{blank}: the optical density of the wells without any cells). All results are presented as mean ± standard error of the mean (SEM) from four independent experiments.

Animal Immunization

Forty-eight healthy 6–8-week-old BALB/c female mice with body weights of 18–21 g were randomly divided into eight groups. Five groups of which mice in 5 groups were immunized intramuscularly in the thigh with 100 μL of each vaccine sample, and the remaining mice in the three groups were injected with ferritin, pCPG, and PBS as negative or blank controls. All mice were boosted with the same vaccines four weeks post-initial vaccination.

Nine 6–8-week-old BALB/c female mice were randomly divided into 3 groups and inoculated by the nanovaccine with 2-, 5- and 10-fold of conventional immunization dose, respectively, for safety assessment in vivo. The immunized mice were fed normally for seven consecutive days to observe whether they are healthy and viable. The mouse serum sample was collected 7 days post immunization (d.p.i.) for biochemical testing.

Blood Biochemical Testing

Whole blood was collected 12 weeks post-immunization (w.p.i.) or 7 d.p.i. from the animals into lithium-heparin or serum tubes (BD Rapid Serum Tubes) and sent to the China Agricultural University Veterinary Teaching Hospital for serum biochemical testing.

Total IgG and IgG Subclasses Determination

The presence of Eg95-specific antibodies was determined using indirect ELISA. In brief, 96-well ELISA plates were coated with 0.1 mL/well Eg95s (1μg/mL in 0.05 M carbonate buffer, pH9.6) and incubated overnight at 4 °C. The plates were blocked with 0.2 mL/well of blocking solution (5% milk in PBS) for 2 h at 37 °C. Subsequently, diluted serum samples were added and incubated for 1 h at 37 °C. After washing with 0.2 mL/well PBST 6 times, 0.1 mL HRP-conjugated goat anti-mouse IgG, IgG1, IgG2a, IgG2b, or IgG3 were added and incubated for 1 hr at 37 °C. After incubation, the plates were washed six times with PBST, 100 μL/well TMB substrate solution was added, and the plates were incubated for 10 min at room temperature. The reaction was stopped by adding 50 μL/well of 2M H_2SO_4, and absorbance was measured at 450 nm using a plate reader.

Splenocyte Isolation

The splenocyte isolation was performed as previously reported.[24] In this case, all mice were euthanized 90 days after the first vaccination, and the spleens were excised and ground through a sterile 60-μm sieve screen to collect single cells. After washing three times with Dulbecco's modified Eagle's medium (DMEM) supplemented with antibiotics-antimycotics, splenocytes were incubated with 200 μL RBC lysis buffer for 3 min at room temperature, and then 1 mL DMEM supplemented with 10% FBS was added to stop the reaction. The cells were centrifuged at 200 g for 5 min, followed by removing the supernatant was removed, and 1 mL DMEM was added to resuspend the cell pellet. After washing twice, the cells were resuspended in 1 mL DMEM, and the number of live cells was counted using 0.2% trypan blue (Gibco-BRL) and an improved Neubauer counting chamber.

Secretion Granzyme B/Cytokine Assays and Splenocyte Proliferation Analysis

The isolated splenocytes were adjusted to a concentration of 2×10^5 cells/mL using DMEM containing 10% FBS, 10 mm HEPES, and 1% antibiotics, and seeded in 96-well plates (0.1 mL/well).

After the cells adhered to plates, Eg95s (10 μg/mL), BSA (10 μg/mL), ConA (5 μg/mL) or RPMI1640 was added, respectively, and incubated for 72 h at 37 °C under 5% CO_2. The supernatants were collected, and the levels of Granzyme B, IFN-γ, IL-4, IL-6, IL-10, and TNF-α were analyzed using a MILLIPLEX MAP mouse $CD8^+T$ cell magnetic bead panel according to the manufacturer's instructions.

After the cells adhered to plates, Eg95s, BSA, ConA, or RPMI1640 was added to plates and incubated for 48 h at 37 °C under 5% CO_2. Next, 10 μL of MTS stock solution was added to each well and incubated for another 3 h under the same conditions. Finally, absorbance was measured at 490 nm using a microplate reader (ELX800 UV, BIO-TEK, USA). The stimulation index (SI) was calculated using the following formula:

$$SI = \frac{ConA \text{ or } BSA \text{ or } Eg95s - Blank}{Control - Blank} \times 100\%$$

Histopathology

Tissue samples recovered from necropsy at 12 weeks post-immunization (w.p.i.) were fixed with 10% neutral-buffered formalin. They were then embedded in paraffin, sectioned, and stained with hematoxylin and eosin (HE).[25] Histological sections were observed under a light microscope.

Statistical Analysis

All values are presented as the mean ± SEM. The statistical significance of the data was evaluated by one-way analysis of variance (ANOVA) using GraphPad Prism 9.0. Statistical significance was set at P-value <0.05.

Results

Expression and Determination of Eg95s-Fe Nanoparticles

The Eg95s Nanoparticle antigen was prepared using the *E. coli* BL21 (DE3) expression system. The Eg95s sequences were fusion-expressed with *Helicobacter pylori* ferritin at the N-terminus (Figure 3A). The fusion subunits self-assembled into 24-mer nanoparticles, and triple monomeric Eg95s as triplets were displayed on the nanoparticle surface, as shown in Figure 3B. After purification, electrophoresis and Western blot analysis showed that the fusion proteins were expressed at the predicted values (Figure 3C), and successful self-assembly of nanoparticles was confirmed by transmission electron microscopy (TEM) and immunoelectron microscopy (IEM) (Figure 3D).

Ferritin Scaffold-Based Nanovaccine Shows High Safety Profiles in vitro and in vivo

In vitro Cytotoxicity by MTS Analysis

RAW 264.7, MDBK, and BHK-21 cells were exposed to various concentrations of adjuvants (potentiators and delivery system) for 24 h. Toxicity profiles were determined using the MTS assay. In general, RAW 264.7 showed the highest sensitivity to adjuvants in all treatments among the three cell types (Figure 4). In the ferritin group, the cell viability remained stable and decreased moderately with treatment from 100 to 400 μg/mL in a dose-dependent manner and remained higher than 60% under the maximum exposure (400 μg/mL) in all cell types (Figure 4A), indicating the high safety of the ferritin scaffold. In the potentiator groups, cell viabilities of RAW 264.7 and BHK-21 began to decline after treatment with 50 μg/mL, while this reduction was alleviated in MDBK cells, starting at 100 μg/mL. Between two potentiators, the cytotoxicity of pCPG was significantly lower than Quil-A at almost all 100, 200, 400 μg/mL treatments in three cell lines except for the treatment with 200 μg/mL in RAW 264.7 cells. Furthermore, the cytotoxicity of ferritin combined with the potentiator pCpG and commercial Quil-A was compared. The combination adjuvant (ferritin + pCpG) still showed lower cytotoxicity than Quil-A, and the significance in BHK-21 cells treated with 200 and 400 μg/mL, in RAW 264.7, cells treated with 100 and 400 μg/mL, and in MDBK cells treated with 100 and 200 μg/mL (Figure 4B–D).
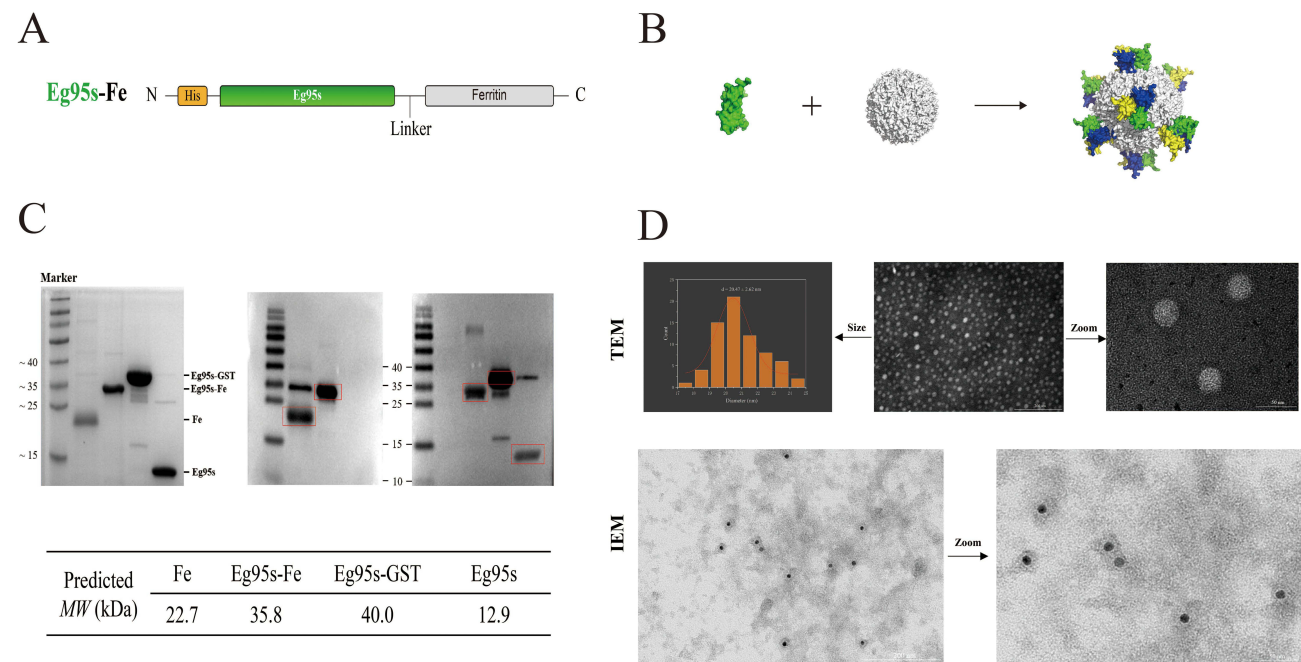
Figure 3 Nanoparticle-based antigen design and characterization. (**A**) The Eg95s sequence containing a 6× His-tag at the N-terminus was ligated to the N-terminus of ferritin via a flexible SGG linker. (**B**) The 3D schematic diagram of Eg95s-Fe nanoparticle was simulated using PyMol based on the ferritin (PDB entry 3BVE) and the 3D structural model of Eg95s predicted by Phyre; three different colors were used to distinguish the three identical copies of Eg95s displayed on the orientations of 3-fold symmetry axes. (**C**) Nanoparticles were validated by SDS-PAGE (left), as well as Western blot with anti-His tag antibody (middle) and the polyclonal antibody obtained from the mice vaccinated with Eg95s-GST-digested Eg95s (right). (**D**) Observation of Eg95s-Fe nanoparticle by TEM and IEM.

These findings show that the combination adjuvant had a high safety profile in vitro, supporting the dose used in this study (Fe: 22.5 μg; pCpG, 10 μg).

Blood Biochemical Testing

Serum samples were collected 12 w.p.i. for biochemical testing. No statistically significant differences in serum levels of alanine aminotransferase (ALT), aspartate aminotransferase (AST), urinary albumin excretion rate (UREA), and creatinine (CREA) were observed among the groups, indicating that the ferritin-based nanoparticle vaccines did not cause any hepatotoxic or nephrotoxic side effects (Figure 5A–D). The additional safety assessment in vivo showed that the overdose-immunized mice in three groups were all alive and healthy, and the serum biochemical indicators of mice even immunized with a 10-fold dose of the nanovaccine were normal (Supplementary Table 1).

Histopathology

Tissue samples were collected from animals in the different groups and subjected to histopathological analysis. As shown in Figure 5E, no obvious lesions or pathological abnormalities were observed in the heart, liver, spleen, lung, kidney, or muscle of mice in any of the groups. In general, these findings indicate that the pCPG-adjuvanted nanovaccine had no toxicological effects in mice under normal immune doses.

The Combination Adjuvant (Fe +pCpG) Enhanced the Eg95-Specific Total Serum IgG Antibody Response

Serum was separated from the collected blood samples of vaccinated mice in all test groups at certain time points, as shown in Figure 6A, and the antibody responses were quantified. No specific antibody responses against Eg95 were observed in the control groups (Fe and pCpG, data not shown) and the negative group (PBS) throughout the immunization process (Figure 6B–F).
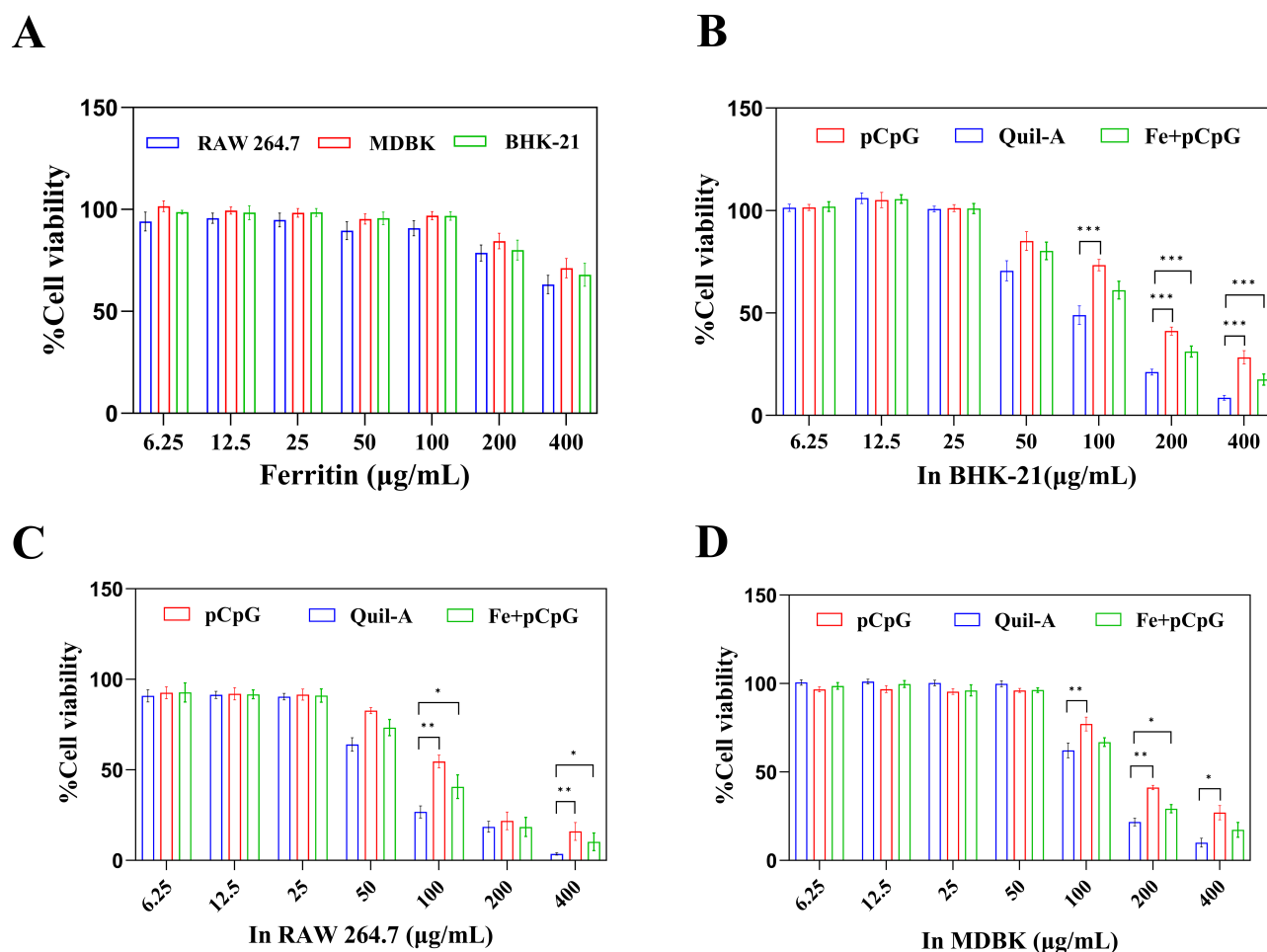
Figure 4 MTS assay cytotoxicity of adjuvants in RAW264.7, MDBK and BHK-21 cells. Cells were treated with ferritin (**A**) Quil-A/pCPG /ferritin+pCpG (**B–D**) at 6.25, 12.5, 25, 50, 100, 200, 400 μg/mL in duplicate wells and plates (n=4) for 24 hrs at 37 °C, cells without adjuvants incubation were used as control, 6.25 in Fe+pCpG group indicates the cells were treated with 6.25 μg/mL of ferritin and pCpG each. After treatment with MTS for 3 hrs, the absorbance at 490 nm was measured and data were calibrated to control readings set at 100%. Data are presented as mean ± SEM. A one-way ANOVA with the student's t test was performed. *$P < 0.05$; **$P < 0.01$; ***$P < 0.005$.

The IgG antibody response induced by vaccines in the different groups (Eg95, Eg95+Quil-A, Eg95-Fe, Eg95+pCpG, and Eg95-Fe+pCpG) showed a similar scenario, that is, the total serum IgG antibody titer began to increase significantly after 4 w.p.i. and peaked at 7 w.p.i. (Figure 6B). From the perspective of adjuvants, all of them alone could significantly improve the IgG antibody level from to 5–12 w.p.i. (Eg95 vs Eg95-Fe/Eg95+pCpG/Eg95+Quil-A); among them, Quil-A exerted higher adjuvanticity between the two potentiators (Eg95+Quil-A vs Eg95+pCpG), whereas, surprisingly, it showed lower adjuvanticity than nanoscaffold ferritin (Eg95+Quil-A vs Eg95-Fe). When ferritin and pCpG were used together as combination adjuvants for the formulation, their immune-enhancing effect on the IgG antibody response was synergistic, as expected. The total IgG response triggered by the Eg95-Fe+pCpG vaccine showed an optimal profile with the earliest production of antibody, the highest antibody titer, and the slowest rate of antibody regression (the longest duration).

The Combination Adjuvant Boosted Antigen-Specific IgG Subclass and Th1 Polarization

Considering that adjuvants may shift the antibody subclass response and that this influence may differ among adjuvants with different modes of action, the titers of the four IgG isotypes in serum were measured (Figure 6C–F). Analysis of the IgG subclass profile showed that the total IgG response in all groups was dominated by IgG1, accompanied by the lowest distribution of IgG3 responses from 4 to 12 w.p.i. (Figure 6B–F). In general, IgG1, IgG2a and IgG2b responses to the
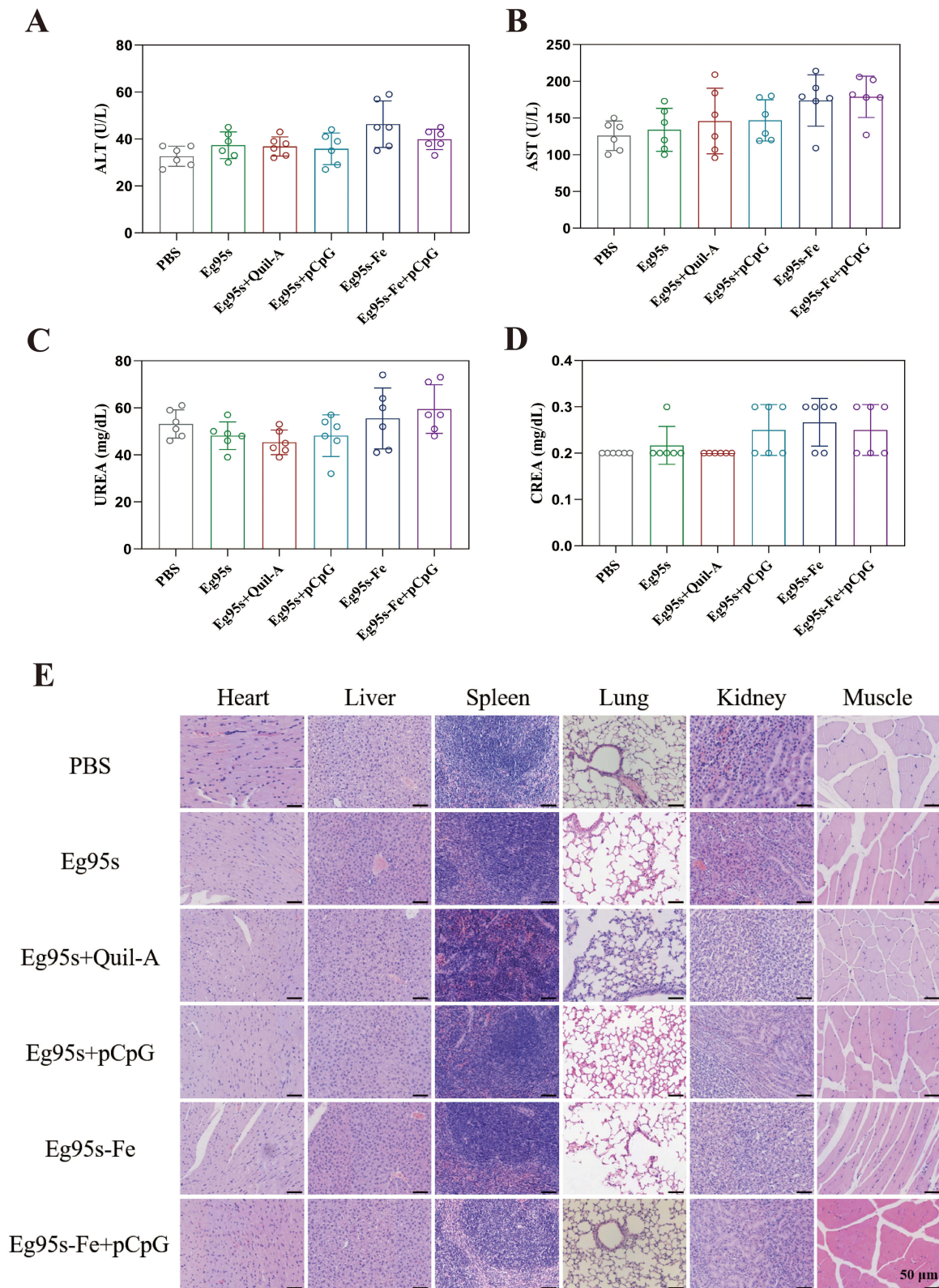
Figure 5 The safety evaluation of nanoparticle-based vaccine in vivo. (**A–D**) Serum biochemical indicators including ALT (**A**), AST (**B**), CREA (**C**) and UREA (**D**), were measured at 12 w.p.i. Data are presented as the mean ± SEM. One-way ANOVA followed by Turkey multiple comparison test was used for statistical analysis. (**E**) Representative images of H&E-stained sections of different organs harvested at 12 w.p.i., scale bar = 50 μm.
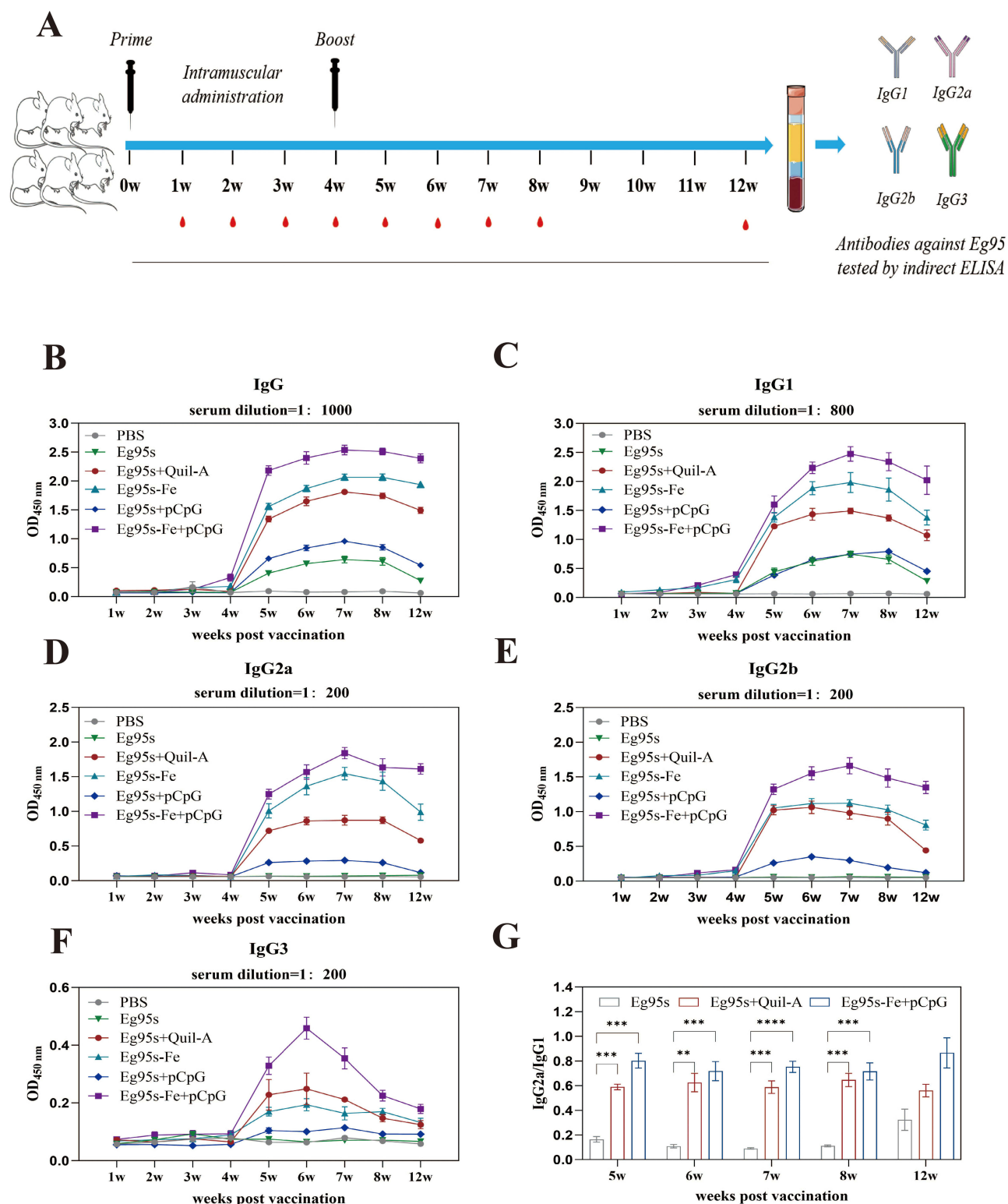
Figure 6 Humoral immune responses specific for vaccines. Schematic of animal experiment and sample preparation (**A**). Total serum IgG (**B**) and four IgG isotypes including IgG1 (**C**), IgG2a (**D**), IgG2b (**E**), IgG3 (**F**) were measured by indirect ELISA in weeks 1, 2, 3, 4, 5, 6, 7, 8, and 12 after primary immunization. (**G**) The ratio of IgG2a/IgG1 was calculated in weeks 5, 6, 7, 8, and 12 after primary immunization. Data are presented as the mean ± SEM. One-way ANOVA followed by Turkey multiple comparison test was used for statistical analysis, **P < 0.01; ***P < 0.005; ****P < 0.0001.

four vaccines (Eg95-Fe+pCpG, Eg95-Fe, Eg95+Quil-A, Eg95+pCpG) presented similar kinetics with those of the total serum IgG antibody, while the differences between IgG and IgG1/2a/2b included: i) pCpG did not showed adjuvant effect on IgG1 response induced by Eg95 (Eg95 vs Eg95+ pCpG) (Figure 6C), ii) single Eg95 hardly induced specific IgG2a and IgG2b responses during 5–12 w.p.i. (Eg95 vs PBS) (Figure 6D and E). For IgG3, the antibody response to Eg95 +Quil-A was more potent than that of the Eg95-Fe group from to 5–12 w.p.i., which showed a reverse outcome compared to the total IgG response (Figures 6B and 5F).

Given that IgG2a is associated with the Th1 immune response, whereas IgG1 is responsible for the Th2 immune response.[26,27] Hence, the IgG2a/IgG1 ratio, which reflects the Th1/Th2 balance, between the positive group (Eg95+Quil-A) and the promising group (Eg95-Fe+pCpG) was also compared at 5–12 w.p.i. As shown in Figure 6G, although Th2 bias (IgG2a/IgG1<1) was observed in all groups at all time points, the IgG2a/IgG1 ratio of the Eg95+Quil-A and Eg95-Fe+pCpG groups was significantly higher than that of the Eg95 group, and this difference was statistically significant at all time points except at 12 w.p.i. Meanwhile, the IgG2a/IgG1 ratio of the Eg95-Fe+pCpG group was obviously higher than that of Eg95+Quil-A. These findings suggested the combination adjuvant could strengthen the Eg95 vaccination by shifting the Th1/Th2 balance much more towards the Th1 response than Quil-A, and this more robust Th1 polarization Eg95-Fe+pCpG induced was believed to further enhance the cellular immune response.[28]

The Combination Adjuvant Enhanced Cellular Immune Responses and Potentiated Th1 Polarization

To assess the effect of adjuvants on immune activation and bias, splenocytes isolated from immunized mice were stimulated with Eg95 antigen, and the levels of Granzyme B and cytokines in the supernatants were determined (Figure 7A). Overall, the production levels of Granzyme B in Eg95-Fe+pCpG and Eg95+Quil-A groups were significantly higher than those in the other four groups ($P < 0.05$) and the secretion level of Granzyme B in Eg95-Fe+pCpG group was 1.23-fold higher than that in the Eg95+Quil-A group ($P > 0.05$). Given that Granzyme B is a serine protease that plays a crucial role in the cytotoxic activity of cytotoxic T lymphocytes (CTLs) and NK cells,[29] and is often used to judge CTL activity, the results of the Granzyme B assay (Figure 7B) indicated that only adjuvant ferritin+pCpG and Quil-A could potentiate CD8$^+$ CTLs activity.

For Th1 cytokines, splenocytes from the Eg95+Quil-A, Eg95-Fe+pCpG, and Eg95+pCpG groups produced almost equal concentrations of the cytokine IFN-γ, which were significantly higher than those from the Eg95 alone group. Meanwhile, Quil-A and pCpG significantly increased the secretion of TNF-α (Eg95+Quil-A vs Eg95, Eg95+pCpG vs Eg95); however, surprisingly, no significant difference was observed between Eg95-Fe+pCpG and Eg95 (Figure 7C). For Th2 cytokines, Quil-A had a better adjuvant effect on the production of IL-4 and IL-6 than the combination adjuvant, whereas Eg95-Fe+pCpG induced a significantly higher level of IL-10 secretion than Eg95+Quil-A (Figure 7D).

Notably, the ratio of the signature Th1 cytokine IFN-γ and Th2 cytokine IL-4 in the Eg95-Fe+pCpG group was significantly higher than that in the Eg95 group (Figure 7E), whereas no significant difference between Eg95+Quil-A and Eg95 was observed. As expected, the trend of Fe+pCpG > Eg95+Quil-A > Eg95 was consistent with the IgG2a/IgG1 profile at 12 w.p.i.

The Combination Adjuvant Potentiated Eg95-Specific Proliferative Response of Splenocytes

To explore the potential underlying mechanisms of adjuvants, antigen-specific T-cell activation and proliferation in vivo using the MTS assay in response to Eg95. As shown in Figure 7F, the proliferation response was specific to Eg95 since stimulation with BSA in vitro had no effect ($P > 0.05$), whereas the proliferation response to Eg95 in spleen lymphocytes isolated from mice immunized with Eg95-Fe+pCpG was significantly higher than that in the other four groups ($P < 0.05$), while the intensity of lymphocyte proliferation stimulated by Eg95+Quil-A was only significantly higher than that of Eg95. Although the difference was not statistically significant ($P > 0.05$), the proliferation response of Eg95 spleen lymphocytes isolated from Eg95-Fe+pCpG immunized mice was higher than that from Eg95+ Quil-A-immunized mice. These data indicate that the proliferation of Eg95-specific T cells could be activated significantly by Fe + pCpG and Quil-A in vivo and that the combination showed stronger stimulating activity at that time.
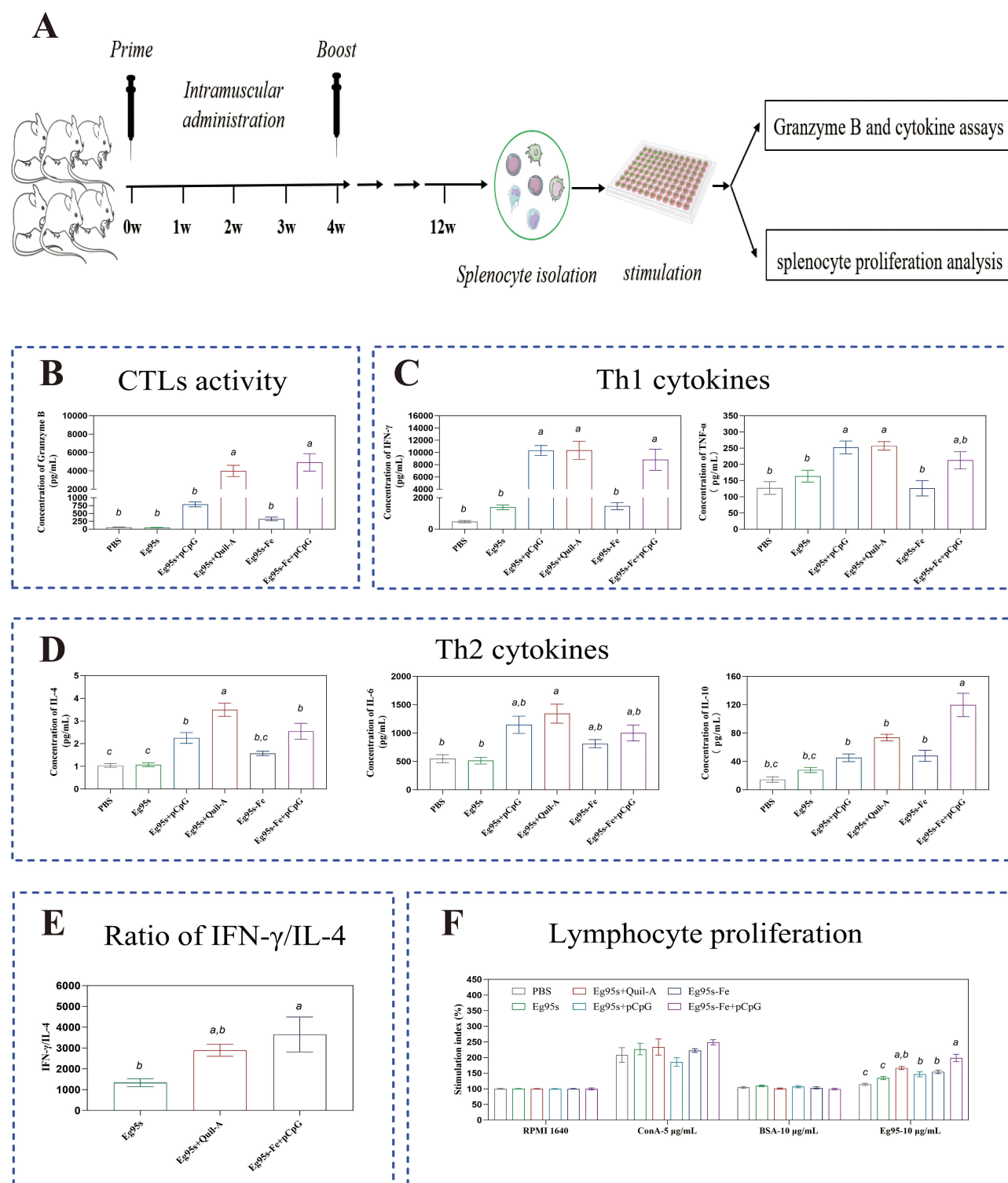
Figure 7 Cellular immune responses triggered by vaccines. Schematic of animal immunization protocol and sample preparation (**A**). The Granzyme B (**B**), Th1 cytokine (**C**), and Th2 cytokine (**D**) were measured by MILLIPLEX MAP mouse CD8^{+} T cell Magnetic bead panel. (**E**) The ratio of signature Th1 and Th2 cytokine. (**F**) Effect of adjuvants on Eg95-specific T cell proliferation. Data are presented as the mean ± SEM. One-way ANOVA followed by Turkey multiple comparison test was used for statistical analysis, different letters indicate statistically significant differences ($P<0.05$).

Discussion

Cystic echinococcosis, a chronic helminth zoonosis, causes huge economic losses to the livestock industry and poses a threat to public health, highlighting the urgency to prevent and control the disease. However, this poses tremendous challenges due to the complexity of the life cycle and extensive genetic diversity.

The Combination Adjuvant Platform Benefits Novel Vaccine Development for Hydatid Disease Control

To date, the precedent for successful CE elimination or control has only occurred in a few limited and isolated small islands (eg, New Zealand) through the vigorous implementation of comprehensive measures, including health education, domestic dog deworming, stray dog disposal, and centralized sheep slaughter.[30,31] For reasons such as geography and Buddhist religious beliefs, relying solely on the New Zealand model to control CE in continental countries such as China will not work.[32] The Eg95 vaccine has proven to be an effective intervention tool against CE disease,[33] and livestock (sheep) vaccination in China has been implemented mandatorily in limited northwestern provinces as a complementary measure and has shown essential effectiveness, contributing to the reduction of livestock CE and minimizing the risk of zoonotic spillover to humans. A recent study by Rong established a dynamic model based on the data from Sichuan province and developed an "if long-term use-can eliminate the disease" optimal control strategy, in which sheep vaccination, as well as dog disposal, were emphasized ahead of domestic dog deworming.[7]

In this study, we offered a safe and viable nanoparticle-based combination adjuvant platform, which is expected to optimize the current vaccine by overcoming the drawback of improving the antigenicity of Eg95 and inducing long-lasting immunity (Figure 6), which makes it possible to reduce the number of immunizations and annual veterinarian visits to the clinic. Meanwhile, it appears that vaccines targeting definitive hosts are more economical and effective for CE control, considering that the number of definitive hosts is less than 1/10 of that of intermediate hosts. If an effective antigen from the worms parasitized in definitive hosts is available, this combination adjuvant platform may have good applicability for the development of a novel canine-target CE vaccine or of universal multivalent "plug-and-display" vaccine against hydatid disease (CE and alveolar echinococcosis) via coupling with the SpyTag/SpyCatcher system.[34]

The pCpG-Adjuvanted Nanovaccine Shows Good Effectiveness and Applicability

The term adjuvant derives from the Latin *adjuvare* meaning help[1] and is commonly defined as an entity incorporated into the formulation to amplify the potency and efficacy of a vaccine.[35] Empirically, adjuvants can be divided into delivery systems and immune potentiators based on the mechanism of action. In 2013, Kanekiyo et al genetically fusion-expressed the antigen to the N-terminus of the ferritin and achieved the stabilization and display of HA on the outer surface of the nanocage; based on the unique structure of ferritin and its self-assembly characteristics, three spatially close HA subunits formed a trimer, thus mimicking the natural conformation of HA; this nanoparticle-based vaccine elicited strong substantial immune response level and broad cross-clade immunity against the influenza.[14] The work ushered a new chapter in ferritin as a remarkable R&D platform for vaccine-used antigens, especially for homo-trimeric structure-class I viral membrane fusion proteins such as HA, Spike, and Evn.[12] Only for spike protein, over 50 studies have been published since the global pandemic of the coronavirus disease 2019.

It is generally believed that nanoparticle-carried antigens have a good deposit effect (retention at the injection site)[36] and long circulation times[37] owing to their size and unique pharmacokinetics in vivo. The size of ferritin, multimerization, and ordered display of antigens on their surface improve the efficiency of antigen uptake and presentation by immune cells,[38,39] which favors the efficient activation of cellular immunity and the induction of specific T cell proliferation,[40] extended germinal center activity, and memory B cell maturation,[41] thereby augmenting the strength and breadth of antigenic immune responses. In this study, a ferritin-based platform was successfully applied to the monomeric antigen Eg95s (Figure 3). The Fe nanoparticle scaffold showed a good auto-adjuvant effect on the humoral immune response, and Eg95s-Fe triggered more potent IgG responses than Eg95s-alone or even the positive control Eg95s+Quil-A (Figure 6B–E). However, the scaffold was unable to potentiate the cellular immune response when certain immune parameters were compared between Eg95s-Fe and Eg95s in Granzyme B and cytokine secretion assays (Figure 7). Combination adjuvants are composed of different components or immunostimulatory

molecules, resulting in synergistic immune activation and induction of a robust immune response. Given that the Th1 response plays an important role in protective immunity against *E. granulosus*,[42] the TLR-9 agonist CpG, a potent Th1 adjuvant, was selected to reinforce the antigenicity of Eg95s-Fe nanoparticles. This Eg95s-Fe + CpG formulation provoked potent and enduring total IgG and isotype antibody responses (Figure 6), sufficient cellular immunity (Figure 7), and more protective immunity-associated Th1 polarization, which may contribute to better protection efficacy and longer protection duration than Eg95s+Quil-A in further clinical trials. In addition to the synergistic and amplified immune activation of the alliance (ferritin + CpG), the cost of this formulation also showed good feasibility and acceptability. First, ferritin is easily produced in *E. coli* at a high yield.[43] Meanwhile, a low-cost, fermentation-produced CpG[20] was used to replace synthetic CpG.

The Drawbacks and Perspectives of the Study

However, animals inoculated with Eg95 vaccine are protected against infection and this protection is highly correlated with the Eg95-specific antibody, which is responsible for the killing of larvae and thus preventing the formation of hydatid cysts.[44] However, a potent and durable antibody response does not fully represent a robust or even complete protective immunity in the clinical. A vaccination-infection experiment in livestock, temporarily absent in this study due to biosafety concerns,[25] should be performed in the future to directly and ultimately evaluate the efficacy and applicability of the vaccine. Meanwhile, the Eg95s-Fe used in this study was mainly from the inclusion body form, and the complex and excessive purification steps were time-consuming and less cost-effective and seemed to affect the correct assembly rate, resulting in suboptimal uniformity of nanoparticle morphology, as observed in Figure 3C. Protein expression in the soluble form needs to be dominant by optimizing the insertion site of the antigen into ferritin[45] and the induction conditions in *E. coli* to save costs.

Conclusion

In summary, the biocompatible and biodegradable ferritin nanoparticle as a delivery platform and an economical derivative of CpG as a potentiator was hybridized and successfully developed as a combination adjuvant for upgrading the current suboptimal Quil-A. In the animal model, the formulated nanovaccine elicited potent and long-term protective immunity, thereby improving the benefit/cost ratio of CE control. This study provides a next-generation CE vaccine as an alternative to the commercial vaccine, and further challenging studies are warranted to verify the efficacy and applicability of this vaccine in the practice of CE control.

Author Contributions

All authors made a significant contribution to the work reported, whether that is in the conception, study design, execution, acquisition of data, analysis and interpretation, or in all these areas; took part in drafting, revising or critically reviewing the article; gave final approval of the version to be published; have agreed on the journal to which the article has been submitted; and agree to be accountable for all aspects of the work.

Funding

Disclosure

The authors declare no conflicts of interest in this work.

References

1. Apostólico Jde S, Lunardelli VA, Coirada FC, Boscardin SB, Rosa DS. Adjuvants: classification, Modus Operandi, and Licensing. *J Immunol Res*. 2016;2016:1459394. doi:10.1155/2016/1459394
2. Romig T, Ebi D, Wassermann M. Taxonomy and molecular epidemiology of Echinococcus granulosus sensu lato. *Vet Parasitol*. 2015;213 (3–4):76–84. doi:10.1016/j.vetpar.2015.07.035

3. Vuitton DA, McManus DP, Rogan MT, et al. International consensus on terminology to be used in the field of echinococcoses. *Parasite*. 2020;27:41. doi:10.1051/parasite/2020024

4. Wen H, Vuitton L, Tuxun T, et al. Echinococcosis: advances in the 21st Century. *Clin Microbiol Rev*. 2019;32(2). doi:10.1128/cmr.00075-18

5. Zhang X, Wei C, Lv Y, et al. EgSeverin and Eg14-3-3zeta from Echinococcus granulosus are potential antigens for serological diagnosis of echinococcosis in dogs and sheep. *Microb Pathog*. 2023;179:106110. doi:10.1016/j.micpath.2023.106110

6. Budke CM, Deplazes P, Torgerson PR. Global socioeconomic impact of cystic echinococcosis. *Emerg Infect Dis*. 2006;12(2):296–303. doi:10.3201/eid1202.050499

7. Rong X, Fan M, Zhu H, Zheng Y. Dynamic modeling and optimal control of cystic echinococcosis. *Infect Dis Poverty*. 2021;10(1):38. doi:10.1186/s40249-021-00807-6

8. Gauci C, Heath D, Chow C, Lightowlers MW. Hydatid disease: vaccinology and development of the EG95 recombinant vaccine. *Expert Rev Vaccines*. 2005;4(1):103–112. doi:10.1586/14760584.4.1.103

9. Cho KJ, Shin HJ, Lee JH, et al. The crystal structure of ferritin from Helicobacter pylori reveals unusual conformational changes for iron uptake. *J Mol Biol*. 2009;390(1):83–98. doi:10.1016/j.jmb.2009.04.078

10. Song N, Zhang J, Zhai J, Hong J, Yuan C, Liang M. Ferritin: a Multifunctional Nanoplatform for Biological Detection, Imaging Diagnosis, and Drug Delivery. *Acc Chem Res*. 2021;54(17):3313–3325. doi:10.1021/acs.accounts.1c00267

11. Georgiev IS, Joyce MG, Chen RE, et al. Two-Component Ferritin Nanoparticles for Multimerization of Diverse Trimeric Antigens. *ACS Infect Dis*. 2018;4(5):788–796. doi:10.1021/acsinfecdis.7b00192

12. Rodrigues MQ, Alves PM, Roldão A. Functionalizing Ferritin Nanoparticles for Vaccine Development. *Pharmaceutics*. 2021;13(10):1621. doi:10.3390/pharmaceutics13101621

13. Mu Z, Wiehe K, Saunders KO, et al. mRNA-encoded HIV-1 Env trimer ferritin nanoparticles induce monoclonal antibodies that neutralize heterologous HIV-1 isolates in mice. *Cell Rep*. 2022;38(11):110514. doi:10.1016/j.celrep.2022.110514

14. Kanekiyo M, Wei CJ, Yassine HM, et al. Self-assembling influenza nanoparticle vaccines elicit broadly neutralizing H1N1 antibodies. *Nature*. 2013;499(7456):102–106. doi:10.1038/nature12202

15. Kanekiyo M, Bu W, Joyce MG, et al. Rational Design of an Epstein-Barr Virus Vaccine Targeting the Receptor-Binding Site. *Cell*. 2015;162(5):1090–1100. doi:10.1016/j.cell.2015.07.043

16. Joyce MG, Chen WH, Sankhala RS, et al. SARS-CoV-2 ferritin nanoparticle vaccines elicit broad SARS coronavirus immunogenicity. *Cell Rep*. 2021;37(12):110143. doi:10.1016/j.celrep.2021.110143

17. Powell AE, Zhang K, Sanyal M, et al. A Single Immunization with Spike-Functionalized Ferritin Vaccines Elicits Neutralizing Antibody Responses against SARS-CoV-2 in Mice. *ACS Cent Sci*. 2021;7(1):183–199. doi:10.1021/acscentsci.0c01405

18. Wang W, Huang B, Zhu Y, Tan W, Zhu M. Ferritin nanoparticle-based SARS-CoV-2 RBD vaccine induces a persistent antibody response and long-term memory in mice. *Cell Mol Immunol*. 2021;18(3):749–751. doi:10.1038/s41423-021-00643-6

19. Chu Y, He Y, Zhai W, et al. CpG adjuvant enhances humoral and cellular immunity against OVA in different degrees in BALB/c, C57BL/6J, and C57BL/6N mice. *Int Immunopharmacol*. 2024;138:112593. doi:10.1016/j.intimp.2024.112593

20. Ren X, Wang X, Zhang S, et al. pUC18-CpG Is an Effective Adjuvant for a Duck Tembusu Virus Inactivated Vaccine. *Viruses*. 2020;12(2):238. doi:10.3390/v12020238

21. Liu X, Song H, Jiang J, et al. Baculovirus-expressed self-assembling SARS-CoV-2 nanoparticle vaccines targeting the S protein induce protective immunity in mice. *Process Biochem*. 2023;129:200–208. doi:10.1016/j.procbio.2023.03.026

22. Lagoutte P, Mignon C, Stadthagen G, et al. Simultaneous surface display and cargo loading of encapsulin nanocompartments and their use for rational vaccine design. *Vaccine*. 2018;36(25):3622–3628. doi:10.1016/j.vaccine.2018.05.034

23. Le Roux G, Moche H, Nieto A, Benoit JP, Nesslany F, Lagarce F. Cytotoxicity and genotoxicity of lipid nanocapsules. *Toxicol In Vitro*. 2017;41:189–199. doi:10.1016/j.tiv.2017.03.007

24. Sun J, Shi J, Li J, et al. The Effect of Immunosuppressive Adjuvant Kynurenine on Type 1 Diabetes Vaccine. *Front Immunol*. 2021;12:681328. doi:10.3389/fimmu.2021.681328

25. Zhao Y, Bi Q, Wei Y, et al. A DNA vaccine (EG95-PT1/2/3-IL2) encoding multi-epitope antigen and IL-2 provokes efficient and long-term immunity to echinococcosis. *J Control Release*. 2023;361:402–416. doi:10.1016/j.jconrel.2023.07.047

26. Barr TA, Brown S, Mastroeni P, Gray D. B cell intrinsic MyD88 signals drive IFN-gamma production from T cells and control switching to IgG2c. *J Immunol*. 2009;183(2):1005–1012. doi:10.4049/jimmunol.0803706

27. Petrushina I, Tran M, Sadzikava N, et al. Importance of IgG2c isotype in the immune response to beta-amyloid in amyloid precursor protein/transgenic mice. *Neurosci Lett*. 2003;338(1):5–8. doi:10.1016/s0304-3940(02)01357-5

28. Liu ZH, Deng ZF, Lu Y, Fang WH, He F. A modular and self-adjuvanted multivalent vaccine platform based on porcine circovirus virus-like nanoparticles. *J Nanobiotechnology*. 2022;20(1):493. doi:10.1186/s12951-022-01710-4

29. Pordanjani PM, Bolhassani A, Pouriayevali MH, Milani A, Rezaei F. Engineered dendritic cells-derived exosomes harboring HIV-1 Nef(mut)-Tat fusion protein and heat shock protein 70: a promising HIV-1 safe vaccine candidate. *Int J Biol Macromol*. 2024;270(Pt 2):132236. doi:10.1016/j.ijbiomac.2024.132236

30. Craig PS, McManus DP, Lightowlers MW, et al. Prevention and control of cystic echinococcosis. *Lancet Infect Dis*. 2007;7(6):385–394. doi:10.1016/s1473-3099(07)70134-2

31. Craig PS, Larrieu E. Control of cystic echinococcosis/hydatidosis: 1863–2002. *Adv Parasitol*. 2006;61:443–508. doi:10.1016/s0065-308x(05)61011-1

32. Heath DD, Jensen O, Lightowlers MW. Progress in control of hydatidosis using vaccination--a review of formulation and delivery of the vaccine and recommendations for practical use in control programmes. *Acta Trop*. 2003;85(2):133–143. doi:10.1016/s0001-706x(02)00219-x

33. Gauci C, Vural G, Oncel T, et al. Vaccination with recombinant oncosphere antigens reduces the susceptibility of sheep to infection with Taenia multiceps. *Int J Parasitol*. 2008;38(8–9):1041–1050. doi:10.1016/j.ijpara.2007.11.006

34. Zakeri B, Fierer JO, Celik E, et al. Peptide tag forming a rapid covalent bond to a protein, through engineering a bacterial adhesin. *Proc Natl Acad Sci U S A*. 2012;109(12):E690–7. doi:10.1073/pnas.1115485109

35. Lee S, Nguyen MT. Recent advances of vaccine adjuvants for infectious diseases. *Immune Netw Apr*. 2015;15(2):51–57. doi:10.4110/in.2015.15.2.51

36. Smith DM, Simon JK, Baker Jr JR. Applications of nanotechnology for immunology. *Nat Rev Immunol*. 2013;13(8):592–605. doi:10.1038/nri3488

37. Hoshyar N, Gray S, Han H, Bao G. The effect of nanoparticle size on in vivo pharmacokinetics and cellular interaction. *Nanomedicine*. 2016;11 (6):673–692. doi:10.2217/nnm.16.5

38. Tokatlian T, Read BJ, Jones CA, et al. Innate immune recognition of glycans targets HIV nanoparticle immunogens to germinal centers. *Science*. 2019;363(6427):649–654. doi:10.1126/science.aat9120

39. Lung P, Yang J, Li Q. Nanoparticle formulated vaccines: opportunities and challenges. *Nanoscale*. 2020;12(10):5746–5763. doi:10.1039/ c9nr08958f

40. Han JA, Kang YJ, Shin C, et al. Ferritin protein cage nanoparticles as versatile antigen delivery nanoplatforms for dendritic cell (DC)-based vaccine development. *Nanomedicine*. 2014;10(3):561–569. doi:10.1016/j.nano.2013.11.003

41. Kelly HG, Tan HX, Juno JA, et al. Self-assembling influenza nanoparticle vaccines drive extended germinal center activity and memory B cell maturation. *JCI Insight*. 2020;5(10):136653. doi:10.1172/jci.insight.136653

42. Paredes R, Godoy P, Rodríguez B, et al. Bovine (Bos taurus) humoral immune response against Echinococcus granulosus and hydatid cyst infertility. *J Cell Biochem*. 2011;112(1):189–199. doi:10.1002/jcb.22916

43. Fan K, Cao C, Pan Y, et al. Magnetoferritin nanoparticles for targeting and visualizing tumour tissues. *Nat Nanotechnol*. 2012;7(7):459–464. doi:10.1038/nnano.2012.90

44. Díaz Á. Immunology of cystic echinococcosis (hydatid disease). *Br Med Bull*. 2017;124(1):121–133. doi:10.1093/bmb/ldx033

45. Fan K, Jiang B, Guan Z, et al. Fenobody: a Ferritin-Displayed Nanobody with High Apparent Affinity and Half-Life Extension. *Anal Chem*. 2018;90(9):5671–5677. doi:10.1021/acs.analchem.7b05217